Available online at www.sciencedirect.com
SCIENCE DIRECT®
Optical Materials 28 (2006) 1047–1053
OPTICAL Materials
www.elsevier.com/locate/optmat

Synthesis and characterization of PVP-encapsulated ZnS nanoparticles

Gopa Ghosh, Milan Kanti Naskar, Amitava Patra *, Minati Chatterjee *

Sol-Gel Division, Central Glass and Ceramic Research Institute, Jadavpur, Kolkata 700 032, India

Received 9 November 2004; accepted 10 June 2005
Available online 20 July 2005

Abstract

We report a simple soft chemical method for the synthesis of PVP-encapsulated ZnS nanoparticles and examine the optical properties of these ZnS nanoparticles with varying ageing time at the reaction temperature, concentrations of PVP and S^{2-} ions. The observed photoluminescence peak of PVP capped ZnS nanoparticles at 407 nm, markedly blue shifted relative to that of the bulk ZnS, clearly indicates the strong quantum size effect. A mechanism for the formation of PVP encapsulated ZnS nanoclusters under varying PVP/Zn^{2+} mole ratio has also been suggested.

1. Introduction

A burst of research activities has been emerged in the synthesis and characterization of semiconductor nanoparticles for size dependent optical properties, because they find great applications in photonic and biophotonics [1–5]. The size dependence of the bandgap is the most identified aspect of quantum confinement in semiconductors; the bandgap increases as the size of the particles decreases. When the dimensions of nanocrystalline particles approach the exciton Bohr radius, a blue shift in energy is observed due to the quantum confinement phenomenon. The effective mass model is commonly used to study the size dependence of optical properties of quantum dots (QD) system. The tunability of the properties of nanoparticles by controlling their size may provide an advantage in formulating new composite materials with optimized properties for various applications. However, applications would be restricted due to different nonradiative relaxations pathways. One of the most important nanoradiative pathways is surface related defects. To overcome the above mentioned difficulties, organic and inorganic capping agents are used to passivate the free quantum dots. Various wet chemical methods have been developed for the synthesis of sulphide nanoparticles [6–10]. To control the growth of the nanoparticles, organic stabilizers (polymers) e.g. polyethylene oxide (PEO), poly(*N*-vinyl-2 Pyrrolidone, PVP), polyvinylcarbazole (PVK) are added during the wet-chemical synthesis for capping the surface of the particles [11–13]. The understanding of the effect of capping on nanoparticles is one of the most important topics now-a-day. The fundamental question that we are attempting to address in this paper is how the capping causes any noticeable improvement of efficiency of nanoparticles.

Keeping the above points in view, we report a simple soft chemical method for the synthesis and characterization of PVP-encapsulated ZnS nanoparticles and the influences of process parameters (i) ageing time at the reaction temperature, (ii) concentration of PVP and (iii) concentration of S^{2-} ions on the efficiencies of ZnS nanoparticles.

* Corresponding authors. Fax: +91 33 24730957.
E-mail addresses: apatra@cgcri.res.in (A. Patra), minati@cgcri.res.in (M. Chatterjee).

0925-3467/$ - see front matter © 2005 Elsevier B.V. All rights reserved.
doi:10.1016/j.optmat.2005.06.003

2. Experimental

2.1. Synthesis of PVP-encapsulated ZnS nanoparticles

The starting materials for the synthesis of ZnS nanoparticles were zinc acetate tetrahydrate (G.R, glaxo laboratories India Ltd.), thiourea (G.R., s.d.fine chem. Ltd.), poly-*N*-vinyl-2-pyrrolidone (PVP, molecular weight 58,000, ACROS, USA) and *N*,*N*-dimethyl formamide (DMF, G.R., Merck, India). PVP was used as the capping agent in the present study. The synthesis reaction was carried in the DMF medium. Calculated quantity of zinc acetate, thiourea and PVP was dissolved in DMF under stirring of 150 rpm in a tightly closed glass container so as to obtain homogeneous solutions. The concentration of Zn^{2+}, S^{2-} and PVP used in the DMF were 7.5×10^{-2} M, 15×10^{-2} M and 5×10^{-4} M, respectively. The container with the reaction solution was thereafter placed in an oil bath, preheated at a temperature of 136 ± 1 °C, for 10 min under constant stirring, removed from the bath and cooled to ambient temperature. The pH of the transparent sol was about 6. The dispersed sulphide nanoparticles were collected from the DMF solution by adding a known volume of acetone (G.R., Merck, India). Immediate flocculation of nanoparticles occurred. Particles were collected using centrifugation at 6000 rpm. To remove the last traces of adhered impurities, the particles were washed thrice using acetone, each time collecting the particles using centrifugation as described above. The washed particles were dried at 60 °C in air. For the measurement of the UV–Vis absorbance and fluorescence spectra, the dried particles were dispersed in conductivity water (conductivity of water: 1.4×10^{-5} mho). Fig. 1 presents a schematic of the formation of PVP- encapsulated ZnS nanoparticles. For the synthesis of uncapped ZnS nanoparticles, the same precursor composition, in the absence of PVP, was used. However, in this case, since no particle formation occurred at pH 6 even after heat-treatment at $136° \pm 1$ °C for 75 min, the pH of the same solution was thereafter increased to 8 by the addition of ammonia solution. Further heating for 2 min at $136° \pm 1$ °C, colloidal particles appeared making the sol turbid. The particles were collected as described above. To examine the effect of process parameters on the characteristics of the synthesized nanoparticles, the same experimental procedure was followed by varying the (i) ageing time at the reaction temperature, (ii) concentration of PVP and (iii) concentration of S^{2-} ions.

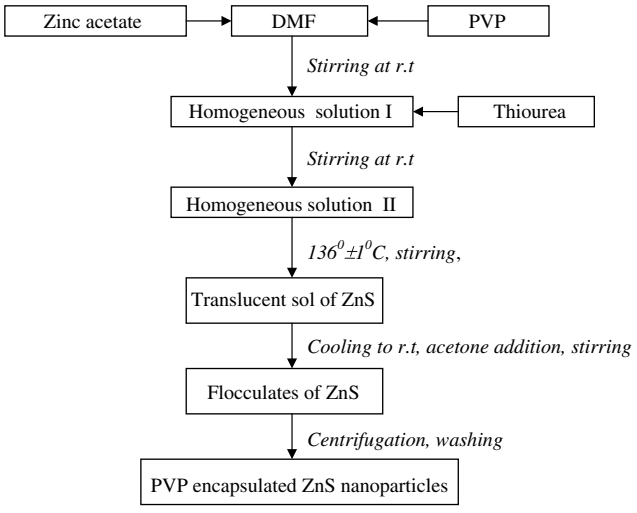

Fig. 1. A schematic of the formation of PVP-capped ZnS nanoparticles.

2.2. Characterization of the sulphide nanoparticles

The ZnS nanoparticles were characterized by X-ray diffraction (XRD) (Model: Philips, 1730, USA) with Ni-filtered CuK_α radiation, FTIR study (Model: Nicolet 5PC, USA), and transmission electron microscopy (TEM) (Model: JEOL JEJ-200X, Japan). Fluorescence spectra of ZnS nanoparticles dispersed in water (conductivity of water: 1.4×10^{-5} mho) were recorded with a spectrofluorimeter (Model: LS 55, Perkin Elmer, USA) in the wavelength range of 200–650 nm. Optical absorbance of the ZnS particles and the PVP were recorded with an UV-Vis spectrophotometer (Model: Cary 50, Varian) in the range 200–550 nm. Crystallite size of ZnS nanoparticles were calculated following the Scherrer's equation,

$$D = K\lambda/\beta\cos\theta \quad (1)$$

where $K = 0.9$, D represents crystallite size (Å), λ, the wavelength of CuK_α radiation and β, the corrected half width of the diffraction peak.

3. Results and discussion

Fig. 2(a) and (b) represent the XRD patterns of PVP-encapsulated and uncapped ZnS nanoparticles, respectively as the typical examples. It is to be noted that, in both the figures the peaks observed in the XRD patterns match well with those of the β-ZnS (cubic) reported in the JCPDS Powder Diffraction File no. 5-0566. Intensities of the three most important peaks of ZnS, namely ⟨1 1 1⟩, ⟨2 2 0⟩ and ⟨3 1 1⟩ reflections corresponding to 28.5°, 47.6° and 56.4° respectively do not deviate from the Powder Diffraction File intensities. Broadening of the XRD peaks indicates the formation of ZnS nanocrystals. It is to be noted that the other samples exhibited the same XRD patterns as presented in Fig. 2. Based on the Scherrer equation, the crystallite size of the nanoparticles were calculated using ⟨1 1 1⟩ reflection of the XRD patterns and estimated sizes are 2.74 nm for

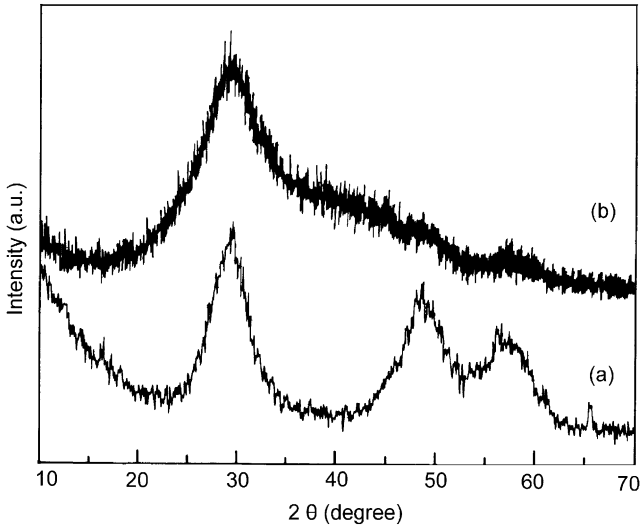

Fig. 2. XRD patterns of uncapped (a) and PVP-capped (b) ZnS nanoparticles.

uncapped ZnS nanoparticles and 1.95 nm for the PVP capped ZnS nanoparticles (PVP/Zn^{2+} mole ratio of 0.007). However, with the increase or decrease in PVP/Zn^{2+} mole ratios from 0.007, the cluster size increases to 2.28 nm. Further, it is to be noted that the effect of ageing time at the reaction temperature has been found to be more pronounced on the formation of nanocrystals compared to the other processing parameters. In this case, the cluster size of ZnS becomes similar to that of the uncapped particles. Therefore, XRD results clearly support the formation of PVP–ZnS nanocomposites. Fig. 3 presents the TEM of ZnS particles obtained in absence of PVP (Fig. 3(a)) and in presence of PVP (Fig. 3(b)). The figure indicates that the PVP capped ZnS nanoparticles (Fig. 3(b)) are monodispersed in nature and the size was estimated to be 2–3 nm which is corroborated with the XRD results. Uncapped nanoparticles (Fig. 3(a)), on the other hand, are agglomerated and quite large in size. This clearly explains the necessity of using the PVP as the capping agent.

FTIR spectra of the PVP only and PVP-capped ZnS are presented in the range 4000–500 cm^{-1} in Fig. 4(a) and (b) respectively. It is to be noted that all the absorption peaks of the PVP in Fig. 4(a) used in the present work, totally matches with those reported in the literature [14]. Further, comparing the FTIR spectra of the PVP and PVP-capped, it is observed that (a) absorption peaks in the range 2959–2879, 1494–1414 and 1374 cm^{-1} are ascribed to the C–H bonding and (b) the strong absorption peaks at around 1659 cm^{-1} and 1295 cm^{-1}, observed in Fig. 4(a) and (b), are assigned to be due to the C–O bonding. Moreover, compared to Fig. 4(a), the decrease in the intensity followed by the increase in broadness of the peaks in the range 2959–2879 cm^{-1}, 1494–1414 cm^{-1} and 1374 cm^{-1} occur in Fig. 4(b). This is believed to be due to the formation of co-ordinate bond between the nitrogen atom of the PVP and the Zn^{2+} ions. Other small peaks are, however, not discussed here. Therefore, the XRD and FTIR studies strongly support the formation of PVP-encapsulated ZnS nanoclusters.

Fig. 5 shows the absorption spectra of PVP-encapsulated and uncapped ZnS nanoparticles, respectively as the typical examples. The absorption edges are 335 and 323 for ZnS uncapped, ZnS capped with PVP, respectively. The blue shift of absorption edge compared to bulk ZnS (onset is at 340 nm) clearly explained by quantum confinement effect of ZnS nanoparticles. The absorption edges of the nanocrystallites are also sharp, indicating that the synthesized particles have relatively narrow size distributions. Here, we calculate the cluster size of ZnS using the following equation [15,16]:

$$\Delta E = \pi^2 h^2/2\mu r^2 - 1.78e^2/\varepsilon r, \quad (2)$$

where ΔE is blue shift band gap and μ is the reduced mass of electron and hole. 0.2 is taken as the electron rest mass m_0, r is the cluster size and ε is the dielectric constant. The first term indicate the confinement effect and the second term being the Coulomb term. In a strong confinement, as in the present case, the second

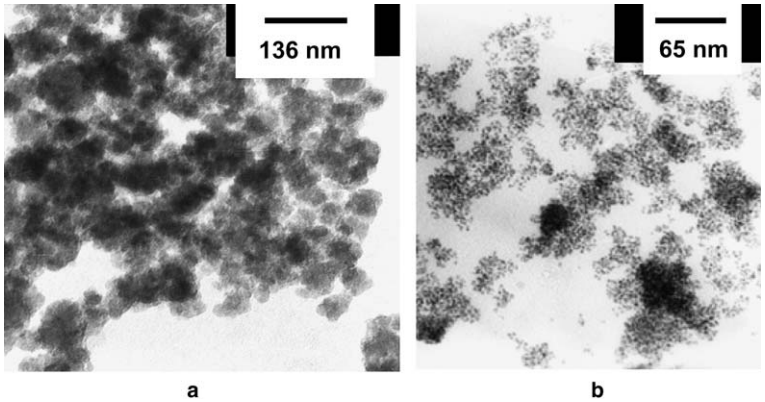

Fig. 3. TEM of uncapped (a) and PVP-capped (b) ZnS nanoparticles.

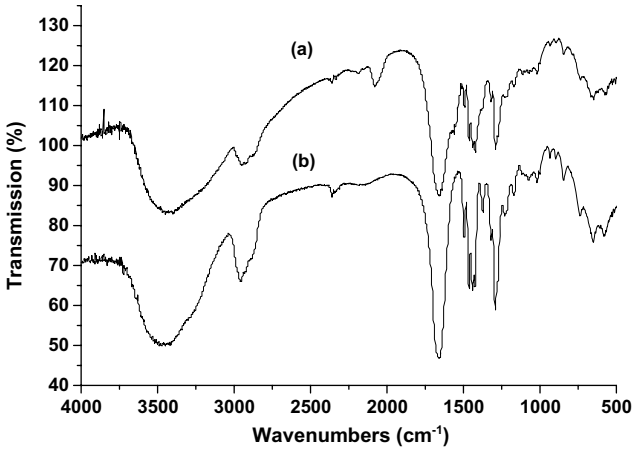

Fig. 4. FTIR spectra of PVP-capped ZnS (a) and PVP only (b).

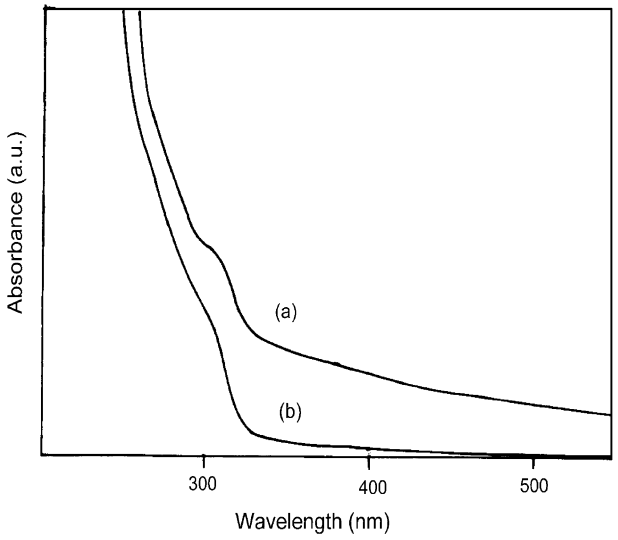

Fig. 5. Absorption spectra of uncapped (a) and PVP-capped (b) ZnS nanoparticles.

term is small and can be neglected. Compared to the capped nanoparticles, the uncapped ZnS (although prepared at some high pH) absorbs at the longest wavelength peaking at 308 nm with the corresponding largest particle size of 2.80 nm. However, the excitonic absorption peak at 297 nm is observed for PVP capped ZnS nanoparticles (PVP/Zn^{2+} mole ratio of 0.007). Because the binding energy of the exciton increases with decreasing size due to an increasing Coulombic overlap enforced by spatial localization of the wave functions as the shift in the band gap with size dominates the spectral changes [10]. This clearly proves the necessity of using the PVP as the capping agent during the synthesis of nanoparticles. Further, it is to be pointed out that the cluster size of ZnS estimated from the optical absorption study are comparable to those obtained from the XRD analysis, although in some cases minor deviations exist. This result reveals that capping of ZnS nanoparticles by PVP causes noticeable influence on the cluster size of the ZnS nanoparticles.

The effect of capping agent on ZnS nanocluster formation has been presented in Fig. 6. Comparing the PL spectra of PVP capped and uncapped ZnS nanoclusters, it is to be noted that the PL spectra of the uncapped particle is quite broad, the peak becomes red shifted to 432 nm and the intensity of the peak decreased three times compared to that of the capped nanoclusters (emission peak at 407 nm). This is expected because in the absence of the capping agent, uncontrolled nucleation and growth of the particles occurred, resulting in the formation of defect states. This result clearly justifies the necessity of using the PVP as the capping agent during the synthesis of ZnS nanoclusters, following the developed technique, of enhanced luminescence properties. Fig. 7 depicts the effect of PVP concentration on the luminescence properties of ZnS nanoclusters. Comparing the three PL spectra of the PVP/Zn^{2+} mole ratios of 0.003, 0.007 and 0.01, respectively, it is worth noting that the maximum PL intensity resulted corresponding to the PVP/Zn^{2+} mole ratio of 0.007 in Fig. 7. Increase or decrease in PVP/Zn^{2+} mole ratio from 0.007 caused a drastic fall in PL intensity making the emission spectra broad and red shifted to the higher wavelength. This result reveals the importance of concentration of PVP. Again, we will examine the effect of different ageing time at the reaction temperature on the photoluminescence spectra of PVP capped ZnS nanoparticles. Fig. 8 shows the photoluminescence spectra of the ZnS nanoparticles prepared at different ageing time at the reaction temperature. The photoluminescence spectrum of PVP capped ZnS nanoparticles ($t = 55$ min) exhibited an emission maximum at 407 nm and this intensity decreases when the ageing time is 60 min at the same reaction tempera-

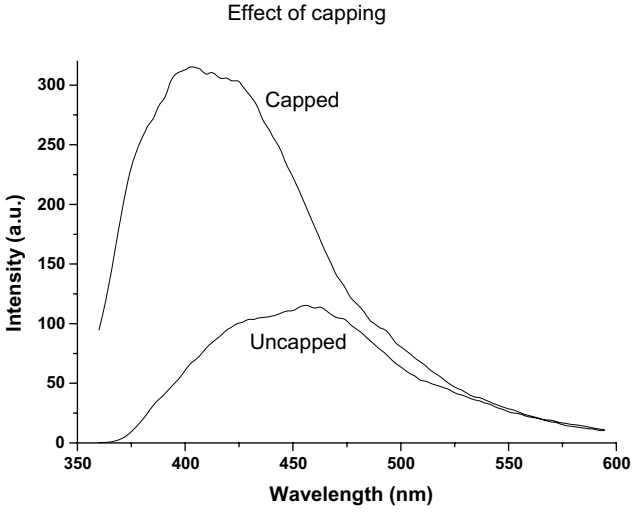

Fig. 6. Photoluminescence spectra of uncapped and PVP-capped ZnS nanoparticles.

ture. The observed photoluminescence peak at 407 nm is markedly blue shifted relative to that of the bulk ZnS (440 nm). It is to be noted that the intensity of the peak maximum decreases with increasing the ageing time at reaction temperature, which indicates that particles size increases, as indicated in Table 1. Further, the common feature in all the PL spectra that the emission maxima are markedly blue shifted relative to that of the bulk ZnS which occur at about 440 nm. This is due to the quantum size effect of the ZnS nanoclusters [16]. The effect of S^{2-} concentration on the emission characteristics of PVP–ZnS nanoclusters are presented in Fig. 9. The figure clearly indicates that with the decrease in S^{2-} concentration, i.e. with the decrease in Zn^{2+}:S^{2-} mole ratio from 1:2 to 1:1, the PL intensity decreases followed by the red shifting of the peak position from 407 nm to 418 nm. The PL peak at 418 nm is assigned to transitions involving interstitial zinc or sulphur atoms [17]. Therefore, for a fixed PVP/Zn^{2+} mole ratio, decrease in S^{2-} content, conversely, the increase in Zn^{2+} concentration resulted in the enhancement of S^{2-} vacancies in the synthesized particles and thus affecting the photoluminescence characteristics. The emission peak is strongly blue shifted (33 nm) compared to that of bulk ZnS. The above results clearly show that role of ageing time at reaction temperature, concentration of PVP and concentration of S^{2-} ions on the efficiency of ZnS nanoparticles.

Fig. 10 presents the structure of the amphiphilic PVP used in the system. In Fig. 10, the pyrrolidone part (hydrophillic) acted as the head group while the poly-

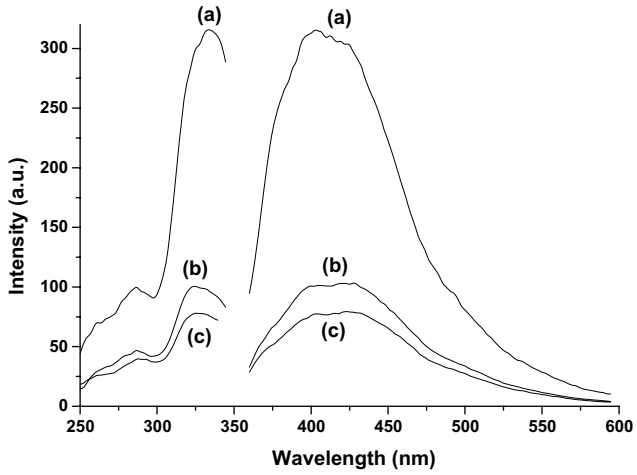

Fig. 7. Photoluminescence spectra of PVP-capped ZnS nanoparticles [PVP/Zn^{2+} mole ratios of 0.007 (a), 0.01 (b) and 0.003 (c)].

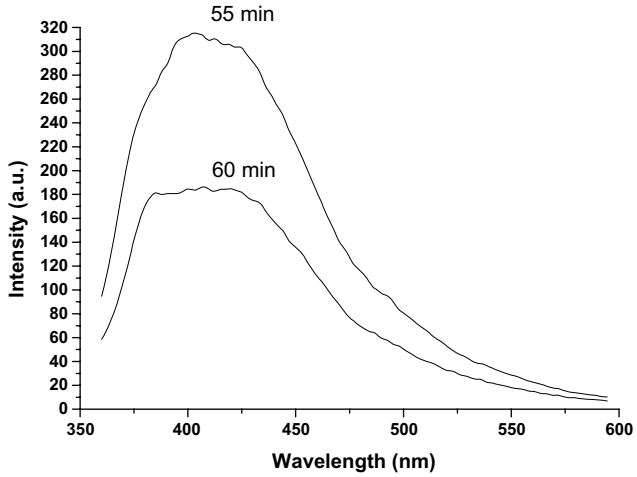

Fig. 8. Photoluminescence spectra of PVP-capped ZnS nanoparticles with different ageing time at same reaction temperature.

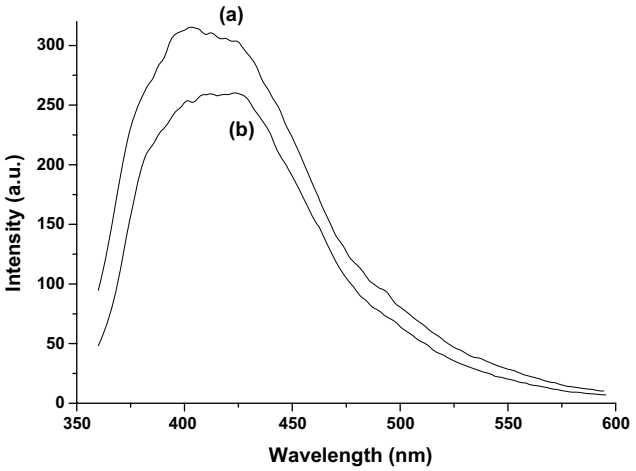

Fig. 9. Photoluminescence spectra of PVP-capped ZnS nanoparticles [Zn^{2+}: S^{2-} mole ratio 1:2 (a) and 1:1 (b)].

Table 1
Calculated cluster size of ZnS nanoparticles from XRD and excitation peak

Samples	Absorption edge (nm)	Excitonic absorption (nm)	Excitonic energy (eV)	Cluster size from (nm)	
				XRD	UV absorption edge
Uncapped ZnS	335	308	4.03	2.74	2.80
PVP/Zn^{2+} (0.007)/55 min	323	297	4.18	1.95	2.36
PVP/Zn^{2+} (0.007)/60 min	328	305	4.07	2.75	2.66
PVP/Zn^{2+} (0.003)	331	302	4.11	2.28	2.54
PVP/Zn^{2+} (0.01)	331	303	4.09	2.28	2.60
Zn^{2+}:S^{2-} mole ratio 1:1	323	298	4.16	2.16	2.41

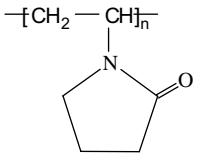

Fig. 10. Molecular structure of PVP.

vinyl part (hydrophobic) acted as the tail group. The role of the PVP is twofold: (a) either it controls the growth of the particles by forming passivation layers around the ZnS core via coordination bond formation between the nitrogen atom of the PVP and Zn^{2+} ion, and/or (b) it prevents agglomeration by steric effect due to the repulsive force acting among the polyvinyl groups (tail part). Therefore, the PVP encapsulation creates a restricted environment around the ZnS nanocrystals. It is found that the molar ratio (0.007) of PVP/Zn^{2+} is most suitable composition for highly efficient ZnS nanoparticles in the present study. When this ratio is less than 0.007, encapsulation of the particles is not effective. On the other hand, when the PVP/Zn^{2+} mole ratio is greater than 0.007, crowding of PVP on the particle surface may cause the attraction among their polymeric chains due to the osmotic pressure difference [18]. This phenomenon is known as 'depletion flocculation', which causes destabilization. It is believed that Zn^{2+} in the reaction medium formed complexed bonds with the nitrogen atom of the PVP. The coordinated Zn^{2+} ions react with the S^{2-} ions, generated via thermal decomposition of thiourea, forming ZnS nanoparticles. In the absence of PVP, Zn^{2+} ions form complex with the sulphur atom of thiourea, thus preventing the availability of H_2S formed via its decomposition even after 75 min of ageing time at 136 ± 1 °C. However, in presence of ammonia solution at pH 8, hydrolysis of thiourea, attached to Zn^{2+} ions, generates H_2S and thus resulting in the rapid formation of agglomerated (uncapped) ZnS particles within 2 min. Here, we propose (Fig. 11) a mechanism for capping of ZnS nanoparticles by PVP. From the above proposed mechanism we infer that (i) the "incomplete encapsulation" (Fig. 10(a)) and "depletion flocculation" (Fig. 10(c)) causes the formation of particle growth followed by a drastic decrease in PL intensity and (ii) the "perfect encapsulation" (Fig. 10(b)) results in the formation of ZnS nanoclusters exhibiting intense PL peak at a wavelength markedly blue shifted compared to those of bulk ZnS.

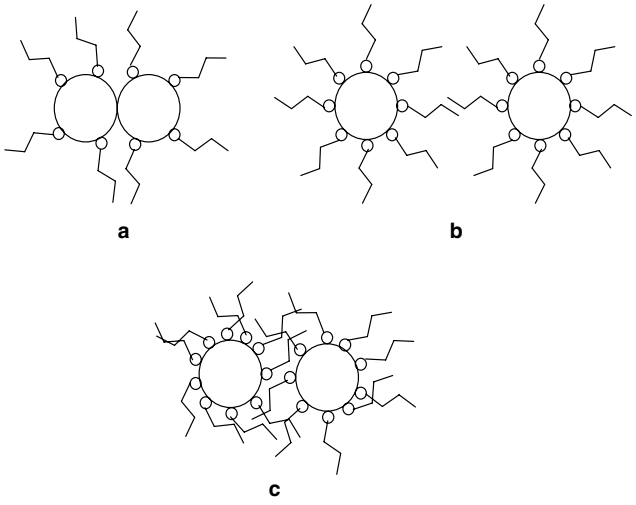

Fig. 11. A schematic showing the effect of PVP concentration on the formation of ZnS nanoparticles: (a) incomplete coverage (PVP/Zn^{2+} molar ratio = 0.003); (b) perfect (optimum) coverage (PVP/Zn^{2+} molar ratio = 0.007) and (c) excess coverage (PVP/Zn^{2+} molar ratio = 0.01).

4. Conclusion

We conclude that the developed soft chemical technique has been proved to be highly efficient for the synthesis of ZnS nanoclusters of enhanced luminescence properties within a very short reaction time. XRD and FTIR studies confirm that PVP could successfully passivate the in situ generated ZnS quantum dots. It has been further proved that the PVP/Zn^{2+} mole ratio played an important role in passivating the nanoclusters, the ratio 0.007 is found to be optimum in the present study. The optical studies show that the absorption and PL peaks of the PVP passivated ZnS nanoclusters are markedly blue shifted compared to those of the bulk ZnS, which clearly indicate the strong quantum size effect. A mechanism for the formation of PVP encapsulated ZnS nanoclusters under varying PVP/Zn^{2+} mole ratio has also been suggested.

Acknowledgments

Authors thank Dr. H.S. Maiti, Director of CGCRI for his constant encouragement and active co-operation to carry out the work. This work is partially financial supported by DST (Project No. III.5(1)/2000-ET).

References

[1] A. Henglein, Chem. Rev. 89 (1989) 1861.
[2] M. Nirmal, L.E. Brus, Science 271 (1996) 933.
[3] M. Bruchez Jr., M. Moronne, P. Gin, S. Weiss, A.P. Alivisatos, Science 281 (1998) 2013.
[4] W.C.W. Chan, S.M. Nie, Science 281 (1998) 2016.
[5] T. Trindade, P. O'Brien, Adv. Mater. 8 (1996) 161.
[6] T. Trindade, P. O'Brien, Chem. Mater. 9 (1997) 523.
[7] M. Azad Malik, P. O'Brien, N. Revaprasadu, J. Mater. Chem. 11 (2001) 2382.
[8] M. Chatterjee, A. Patra, J. Am. Ceram. Soc. 84 (2001) 44.

[9] N. Arul Dhas, A. Gedanken, Appl. Phys. Lett. 72 (1998) 2514.
[10] J. Nanda, S. Sapra, D.D. Srama, N. Chandrasekharan, G. Hodes, Chem. Mater. 12 (2000) 1018.
[11] R. He, X.-F. Qian, J. Yin, H.-a. Xi, L.-J. Bian, Z.-k. Zhe, Colloids Surf. A: Phys. Eng. Aspects 220 (2003) 151.
[12] Y. Yang, H. Chen, X. Bao, J. Cryst. Growth 252 (2003) 251.
[13] K. Roy Choudhury, M. Samoc, A. Patra, P.N. Prasad, J. Phys. Chem. B 108 (2004) 1556.
[14] S. Ganesan, J. Felo, M. Saldana, V.F. Kalasinsky, M.R. Lewin-Smith, J.F. Tomashefski Jr., Mod. Pathol. 16 (2003) 286.
[15] A.B. Yoffe, Adv. Phys. 42 (1993) 173.
[16] J.X. Yin, J. Yan, Z. Zhi-lin, S.-H. Xu, J. Cryst. Growth 191 (1998) 692.
[17] D. Denzler, M. Olschewski, K. Sattler, J. Appl. Phys. 84 (1998) 2841.
[18] R.G. Horn, J. Am. Ceram. Soc. 73 (1990) 1117.